Lukas, R. J., & Bennett, E. L. (1979b) *FEBS Lett. 108*, 356–358.
Lukas, R. J., & Bennett, E. L. (1980a) *J. Biol. Chem. 255*, 5573–5577.
Lukas, R. J., & Bennett, E. L. (1980b) *Mol. Pharmacol. 17*, 149–155.
Lukas, R. J., Morimoto, H., & Bennett, E. L. (1979) *Biochemistry 18*, 2384–2395.
Lukas, R. J., Morimoto, H., Hanley, M. R., & Bennett, E. L. (1981) *Biochemistry 20*, 7373–7378.
Lukasiewicz, R. J., & Bennett, E. L. (1978) *Biochim. Biophys. Acta 544*, 294–308.
Lukasiewicz, R. J., Hanley, M. R., & Bennett, E. L. (1978) *Biochemistry 17*, 2308–2313.
Morley, B. J., & Kemp, G. E. (1981) *Brain Res. Rev. 3*, 81–104.
Schmidt, J., & Raftery, M. A. (1973) *Anal. Biochem. 52*, 349–354.
Schmidt, J., Hunt, S. P., & Polz-Tejera, G. (1980) in *Neurotransmitters, Receptors and Drug Action* (Essman, W. B., Ed.) pp 1–65, Spectrum, New York.
Speth, R. C., Chen, F. M., Lindstrom, J. M., Kobayashi, R. M., & Yamamura, H. I. (1977) *Brain Res. 131*, 350–355.

Detection of Low-Affinity α-Bungarotoxin Binding Sites in the Rat Central Nervous System†

Ronald J. Lukas

ABSTRACT: The curaremimetic neurotoxin, α-bungarotoxin, is shown to interact with two classes of binding sites on rat brain crude mitochondrial fraction membranes. Toxin binding sites are characterized by descriptive, preequilibrium dissociation constants of about 5 and 400 nM. There are at least as many low-affinity toxin binding sites as high-affinity sites. The existence of low- and high-affinity sites is confirmed by experiments with native toxin. Low- and high-affinity toxin binding sites are copurified as judged by sedimentation velocity and density gradient analysis, consistent with the presence of low- and high-affinity toxin binding sites on the same subcellular membrane fragments. The results may offer an explanation for the relatively low antagonistic potency of curaremimetic neurotoxins at acetylcholine-sensitive sites in the vertebrate central nervous system.

Use of curaremimetic neurotoxins as molecular probes in characterization of nicotinic acetylcholine receptors (nAcChoR)[1] in the periphery (Conti-Tronconi & Raftery, 1982) is founded on demonstration of their potent antagonistic action (at submicromolar concentrations) at the vertebrate neuromuscular junction and on the electric organ of ray and eel (Lester, 1970; Lee, 1972). Application of neurotoxins as probes for autonomic and central nervous system nAcChoR (Moore & Loy, 1972; Greene et al., 1973; Salvaterra & Moore, 1973; Simantov & Sachs, 1973; Eterovic & Bennett, 1974; Romine et al., 1974), however, predated rigorous tests of their physiological potency in the autonomic nervous system (ANS) or central nervous system [CNS; see Morley & Kemp (1981) but see also Chou & Lee (1969)]. A review of the literature indicates that curaremimetic neurotoxin antagonistic potency at some loci in the ANS and CNS is reduced, but finite and significant (see Discussion). That is, only at 1–10 μM α-bungarotoxin (Bgt) is the response to acetylcholine (AcCho) or stimulation of cholinoceptive elements blocked (Fex & Adams, 1978; Dun & Karczmar, 1980; Marshall, 1981; Syapin et al., 1982).

Due to technical difficulties and limitations in signal to noise ratios, studies of ANS and CNS Bgt binding have focused on high-affinity sites with apparent dissociation constants on the order of 1 nM. A number of studies have shown that occupation of these sites is inadequate to block putative cholinoceptive responses in the mammalian CNS or ANS (see Discussion). Any attempt to resolve this apparent discrepancy in toxin antagonistic potency and binding site specificity requires coincident study of Bgt binding to sites with relatively low affinity for toxin. For example, if there exist toxin binding sites with an apparent dissociation constant on the order of 100 nM, one would predict occupation of 91 and 99% of those sites at toxin concentrations of 1 and 10 μM, respectively, which may provide detectable expression of toxin-mediated antagonism.

Using freshly prepared ^{125}I-labeled monoiodinated α-bungarotoxin (I-Bgt), and a centrifugation assay with Simonsen-Albino rat brain crude mitochondrial fractions, we have detected a class of Bgt binding sites with relatively low affinity for toxin [see Lukas (1984)]. Data are presented in this paper that further characterize this class of toxin binding sites.

Experimental Procedures

Purification and iodination of Bgt, characterization of radiolabeled toxin, and preparation of rat brain crude mitochondrial fraction membranes are described elsewhere (Lukas, 1984). The general outline of I-Bgt binding and kinetics assays, density gradient centrifugation and sedimentation velocity experiments, affinity-labeling protocols, and preincubation and coincubation ligand competition experiments are also according to procedures detailed in other papers (Lukas

† From the Division of Neurobiology, Barrow Neurological Institute, Phoenix, Arizona 85013. *Received June 20, 1983.* This work was supported by National Institutes of Health Grant NS-16821 and by the Men's and Women's Boards of the Barrow Neurological Foundation.

[1] Abbreviations: nAcChoR, nicotinic acetylcholine receptor; ANS, autonomic nervous system; CNS, central nervous system; Bgt, α-bungarotoxin; AcCho, acetylcholine; I-Bgt, ^{125}I-labeled monoiodinated α-bungarotoxin; d-TC, *d*-tubocurarine.

0006-2960/84/0423-1160$01.50/0

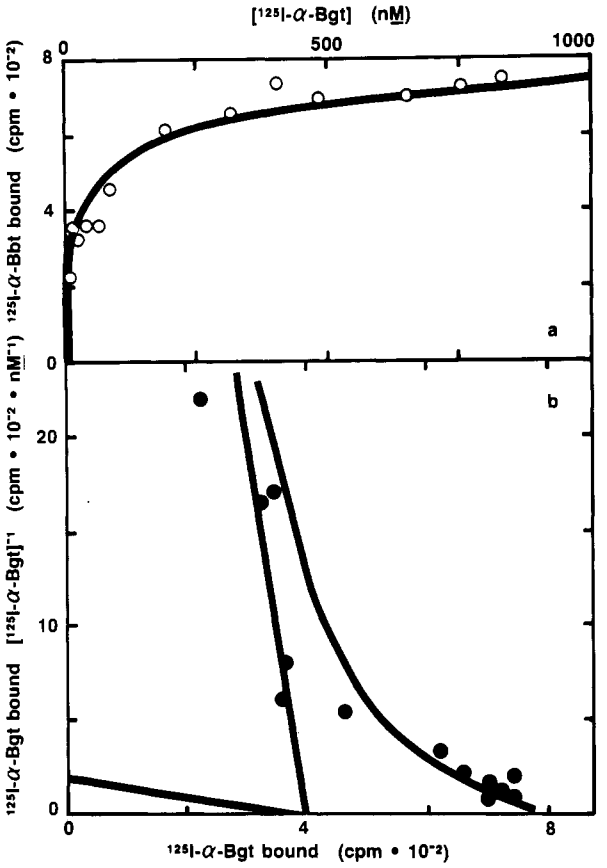

FIGURE 1: I-Bgt saturation profile. Data points for specific I-Bgt (3.8 cpm/fmol) binding to rat brain crude mitochondrial fractions are plotted (a) against final toxin concentration (250-μL assay volume) or (b) in a modified Hofstee–Eadie–Scatchard form. Nonspecific binding (not shown) is linearly related to toxin concentration by the formula cpm bound = 2.8[T], where [T] is the concentration of toxin in nanomolar. Errors in specific binding measurements are typically ±10%. Solid, curved lines are fit to the data by reiterative methods using theoretical curves[2] conforming to $v = V'_1[T](\bar{K}'_1 + [T])^{-1} + V'_2[T](\bar{K}'_2 + [T])^{-1}$, where v is the observed quantity of specific binding and V'_1 and $\bar{K}'_1$ and V'_2 and $\bar{K}'_2$ are the apparent maximum binding levels and dissociation constants for binding with toxin sites 1 and 2, respectively. Parameters used in generating the theoretical curves [and the composite, linear solid lines in (b)] are $V'_1 = V'_2 = 400$ cpm, $\bar{K}'_1 = 5$ nM, and $\bar{K}'_2 = 200$ nM.

et al., 1979; Lukas & Bennett, 1980; Lukas, 1984). Any modifications and details pertaining to toxin or ligand concentrations used are specified in figure or table legends or in the text.

Experimental Design. Nonlinear Scatchard-type plots may arise from technical artifacts due to heterogeneity of radioligand or improper definition of specific binding (Molinoff et al., 1981). While the former possibility can be discounted [see Lukasiewicz et al. (1978), Lukas (1984), and Figure 2], experimental design is critical in eliminating misinterpretation of total and nonspecific binding data. For I-Bgt binding assays described herein, total (test) binding samples are brought to the same final concentrations of radiotoxin and competitor as nonspecific binding (blank) samples. On the basis of the assumption that nonspecific or "falsely specific" binding is quickly dissociable, this ensures that any increase or decrease in such binding in blank samples is compensated for by addition of competitor (chase) to test samples. The only difference between test and blank samples should be due to long-lived radiotoxin binding to sites that are blocked in a long-lived manner by native toxin, or by other cholinergic ligands. Use of the chase procedure and use of a significantly long centrifugation assay may, nevertheless, contribute to a systematic underestimate of binding to low-affinity sites, in

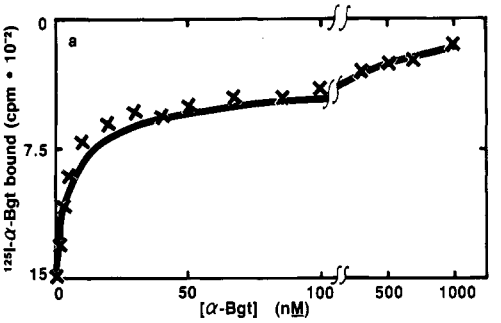

FIGURE 2: Native toxin saturation profile. I-Bgt specific binding is plotted (note inverse y axis) against concentration of native toxin used for pretreatment of membrane sites prior to incubation with 400 nM I-Bgt. The solid line represents the theoretical curve for native Bgt binding to high-affinity (5 nM = $\bar{K}'_1$) and low-affinity (400 nM = $\bar{K}'_2$) sites at equal stoichiometry, which are occupied at 99.8 and 50% capacity, respectively, in the presence of 400 nM radiotoxin.

that low-affinity site–radiotoxin complexes are dissociating as samples are processed. Therefore, values of $\bar{K}'$ for low-affinity toxin binding should be interpreted as descriptive nonequilibrium dissociation constants, in accordance with earlier treatments of the data [see Lukas (1984)].[2]

Results

Toxin-Sensitive Low-Affinity Binding. In a previous publication (Lukas, 1984), I-Bgt saturation curves were displayed, out to a concentration of 100 nM toxin, that suggested the presence of a low-affinity toxin binding component.[2] Illustrated in Figure 1a is a saturation isotherm for native toxin sensitive, specific radiotoxin binding carried out to a concentration of I-Bgt of 840 nM, with a homogeneous preparation of monoiodinated toxin at a specific activity of 3.8 cpm/fmol. Examination of the data reveals that specific binding rises rapidly as radiotoxin concentration increases from 0 to 20 nM, and more gradually from 20 to 500 nM, before approaching an asymptotic limit at higher concentrations of radiolabel. The data are represented in Figure 1b in a modified Hofstee–Eadie–Scatchard form. The solid lines drawn through the data points are theoretical curves based on a 1:1 stoichiometry between high- and low-affinity sites, characterized by $\bar{K}'$ values of 5 and 200 nM, respectively.

In order to confirm these results, and to provide evidence to discount the possibility that the apparent toxin binding site heterogeneity is attributable to heterogeneity of radiolabel, an experiment was performed wherein toxin sites were pretreated with native toxin at various concentrations before incubation with 400 nM I-Bgt. When the data are plotted as shown in Figure 2, a saturation isotherm for native toxin binding to sites capable of interaction with I-Bgt results. The characteristic, rapid initial rise in native toxin binding, followed by a more gradual increase in apparent binding, is evinced as native toxin concentration increases. The solid line drawn through the data represents a theoretical curve for binding of native toxin to high- and low-affinity sites, characterized by $\bar{K}'$ values of 5 and 400 nM, respectively, that are ordinarily 99.8 and 50% occupied by radiolabeled Bgt at the test concentration.

A related experimental paradigm was used to test for independence of low- and high-affinity toxin binding sites. The

[2] An earlier publication (Lukas et al., 1979) should be consulted for derivation of equations describing slowly reversible binding of a toxin to specific binding sites under preequilibrium conditions. The theoretical treatment provides definitions for the descriptive constants used throughout this paper, addresses modification of toxin binding in the presence of competitors, and provides justification for the graphical representations and analyses of data that are presented herein.

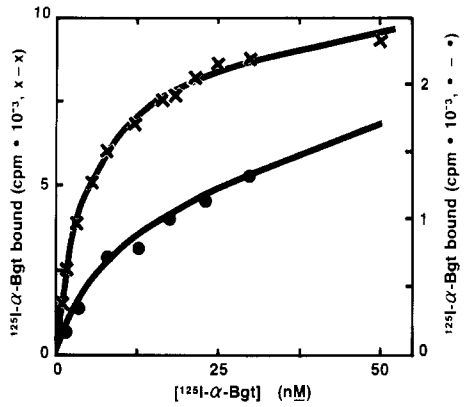

FIGURE 3: Toxin binding site fractional occupancy. Data points represent I-Bgt specifically bound to samples treated with 50 nM native Bgt (●) or buffer only (×) prior to initiation of I-Bgt binding saturation assay at the indicated radiotoxin concentration. Theoretical curves drawn through the data are for binding described by the equation in the legend to Figure 1 for $V'_1 = V'_2 = 9400$ cpm, $\bar{K}'_1 = 5$ nM, and $\bar{K}'_2 = 400$ nM (×) and where 91 and 11% of available high- and low-affinity sites have been blocked by native toxin pretreatment (●). Note the scale differences for each set of data.

upper curve in Figure 3 represents data for I-Bgt binding to rat brain membranes, which is fit with a theoretical curve (solid line) for toxin binding to high- and low-affinity sites with $\bar{K}'$ values of 5 and 400 nM, respectively. The data points in the lower portion of Figure 3 (note scale change on the ordinate) are for radiotoxin binding to sites pretreated with 40 nM native Bgt, which should block 91% of high-affinity sites and 11% of low-affinity sites. The data are fit with a theoretical curve (solid line) for I-Bgt binding to the residual 9 and 89%, respectively, of high- ($\bar{K}' = 5$ nM) and low- ($\bar{K}' = 400$ nM) affinity sites.

Kinetic parameters for radiotoxin binding to toxin-sensitive, low-affinity sites were estimated from association and dissociation experiments (Figure 4). Dissociation of I-Bgt from high-affinity sites (labeled at 5 nM radiotoxin) is characterized by a half-time of ~26.5 h. When membranes are incubated with 250 nM I-Bgt (which should occupy 98% of available high-affinity sites and 38% of available low-affinity sites) and washed free of unbound toxin, approximately 30% of total radiolabel dissociates rapidly, and the remaining 70% of toxin binding site–radiotoxin complexes dissociate with a 26.5-h half-life. When membranes pretreated with 40 nM native toxin (which should block 91% of high-affinity sites and 11% of low-affinity sites) are subsequently treated with 250 nM I-Bgt, the rapidly dissociating component of toxin binding site–radiotoxin complexes comprises approximately 75% of total binding, and 25% of sites dissociate with $\tau_{1/2} = 26.5$ h. From these data, a half-time of ~1 h can be estimated for the dissociation of low-affinity binding site–toxin complexes, yielding $k_{-1} \simeq 1.2 \times 10^{-2}$ min^{-1}. In Figure 4b is illustrated an association rate transform for binding of 250 nM I-Bgt to low-affinity sites (95% of high-affinity sites having been blocked by treatment with 100 nM native Bgt). The data yield a value for k_{obsd} of 1.3×10^{-2} min^{-1} and $k_1 = 5.2 \times 10^{-5}$ min^{-1} nM^{-1}. Thus, the apparent microscopic K_D for low-affinity binding of I-Bgt ($k_{-1}\ k_1^{-1}$) is 230 nM.

Other features of low- and high-affinity toxin binding components are suggested by the results of preincubation competition experiments with AcCho and *d*-tubocurarine (d-TC) and coincubation competition experiments using native Bgt. Values of IC_{50} for AcCho, d-TC, and Bgt are 15 μM, 20 μM, and 25 nM, respectively, for competition toward 10 nM I-Bgt and 100 μM, 200 μM, and 600 nM for competition

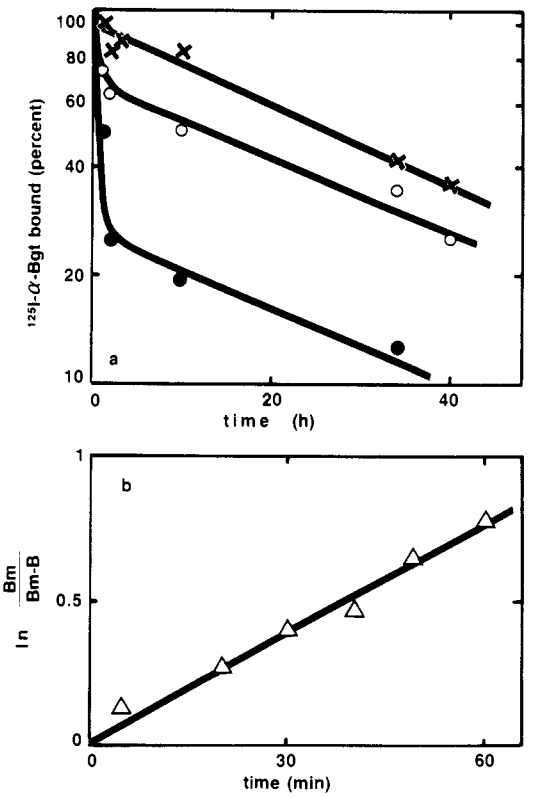

FIGURE 4: Kinetics of low-affinity, toxin-sensitive binding. (a) Dissociation of I-Bgt from toxin–toxin binding site complexes labeled at 5 nM I-Bgt (×) or at 250 nM I-Bgt for samples pretreated with 0 (○) or 40 nM (●) native toxin. (b) Toxin association rate data are plotted as ln [(sites bound at 12 h)(sites bound at 12 h – sites bound at time t)$^{-1}$] against time. Data points represent the difference between binding rate data at 250 nM I-Bgt taken with native membranes and with membranes treated with 100 nM native toxin.

toward 500 nM radiotoxin. However, when radiotoxin at 500 nM is used to label low-affinity sites (after 95% of high-affinity sites are blocked by pretreatment with 100 nM native toxin), IC_{50} values for competition with AcCho and d-TC are between 1 and 10 μM, while IC_{50} values for native toxin are similar to IC_{50} values for competition toward radiotoxin binding to all available low- and high-affinity sites. The data may be interpreted by using the general form of the equation $K_i = IC_{50}(1 + T/K_D^T)^{-1}$, where K_i is the inhibition constant for competing ligand interaction with the toxin binding site(s), T is the concentration of radiotoxin, and K_D^T is the apparent dissociation constant for radiotoxin binding under the conditions of the assay. The results are consistent with a value of $K_i \simeq 1$–2 μM for AcCho and d-TC binding to either low- or high-affinity toxin binding sites, while both K_i for Bgt binding and K_D^T for I-Bgt binding reflect heterogeneity of toxin binding sites.

Toxin-Resistant Low-Affinity Binding. The amount of I-Bgt bound to membrane samples that have been preincubated with supramillimolar concentrations of cholinergic ligands is significantly lower than that for samples preincubated with 1 μM native Bgt, providing a consequent apparent increase in "specific", low-affinity I-Bgt binding. Detailed characterization of this toxin-resistant, low-affinity binding is described and discussed in the supplementary material (see paragraph at end of paper regarding supplementary material).

Physical Disposition of Low-Affinity Toxin Binding Sites. Physical properties of membrane sites that bind I-Bgt with high affinity, sites that bind I-Bgt with low affinity in a toxin-sensitive manner, and sites that bind radiotoxin with low affinity but show toxin resistance were studied. Crude rat

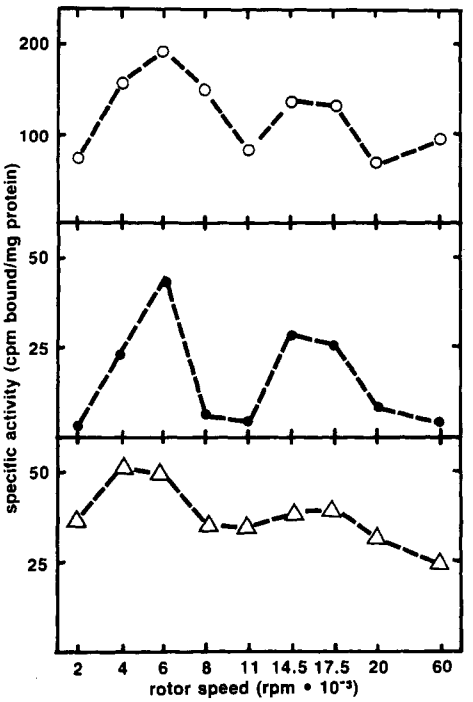

FIGURE 5: Sedimentation velocity profiles of I-Bgt specific binding sites. Specific radiotoxin binding is illustrated for high-affinity [at 5 nM radiotoxin, (○)], for low-affinity, toxin-sensitive [at 400 nM I-Bgt, (●)], and for low-affinity, toxin-resistant [400 nM I-Bgt, (△)] binding, charted as a function of rotor speed used to pellet each fraction.

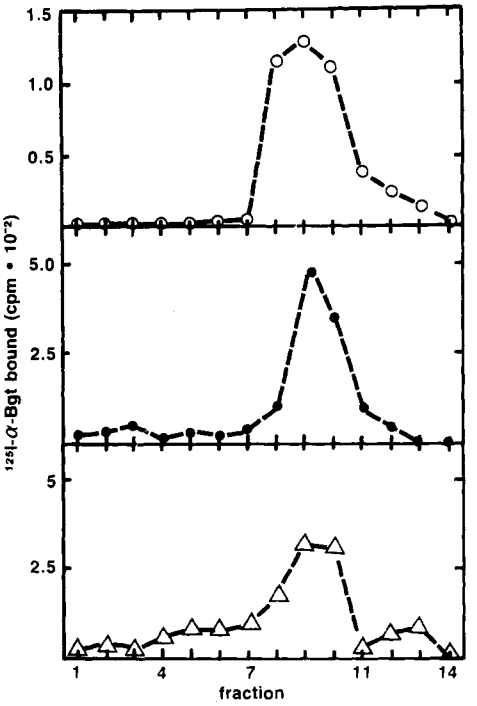

FIGURE 6: Density gradient profiles of I-Bgt binding sites. Crude mitochondrial fraction membranes labeled for high-affinity (○), low-affinity, toxin-sensitive (●), and low-affinity, toxin-resistant (△) binding are resuspended in buffer. Aliquots (2.5 mL) of samples are mixed with 5 mL of isoosmolar Pecoll and 15 mL of buffer to yield Percoll at a density of 1.04 g/mL. Gradient material is subjected to centrifugation at 14 500 rpm for 30 min in the Sorvall SM-24 rotor prior to fractionation.

brain homogenates were fractionated on the basis of sedimentation velocity behavior, and each fraction was assessed for toxin binding activity (Figure 5). Highest levels of high-affinity binding, toxin-sensitive low-affinity binding, and toxin-resistant low-affinity binding occur in the same sedimentation velocity fractions. However, background levels of toxin-resistant low-affinity binding are more generally dispersed across the sedimentation velocity profile than those for toxin-sensitive binding.

Percoll density gradient profiles of specific toxin binding (Figure 6) are also similar for high-affinity binding, toxin-sensitive low-affinity binding, and toxin-resistant low-affinity binding.

Discussion

CNS Bgt binding sites from avian and amphibian sources have been characterized biochemically (Oswald & Freeman, 1981; Norman et al., 1982), and there is good electrophysiological evidence that CNS nicotinic transmission may be blocked by submicromolar Bgt in these nonmammalian systems (Oswald & Freeman, 1981). Curaremimetic neurotoxins are also potent at submicromolar concentrations as nicotinic antagonists at the neuromuscular junction (Lester, 1970), where their biochemical utility is well-established (Conti-Tronconi & Raftery, 1982). In the mammalian ANS and CNS, early reports indicated a lack of toxin potency at cholinergic synapses [see the comprehensive and thoughtful review by Schmidt et al. (1980)]. However, recent studies demonstrate reduced, but finite, antagonistic potency of 1–10 μM Bgt at mammalian CNS cholinoceptive sites (Fex & Adams, 1978; Zatz & Brownstein, 1981; Syapin et al., 1982) and in the frog (Marshall, 1981) and rat (Dun & Karczmar, 1980) autonomic nervous system.

Earlier (Lukas, 1984), we presented data indicating detection in the rat CNS of low-affinity binding sites for radioiodinated Bgt and *Naja naja siamensis* toxin. Those results have been confirmed and extended in this paper. The present data demonstrate that saturation of a low-affinity binding site ($\bar{K}' \simeq$ 200–400 nM) for I-Bgt on rat brain membranes may be approached at radiotoxin concentrations of ~1 μM. These results are confirmed in experiments using native Bgt as well as radiolabeled toxin. The microscopic dissociation constant for low-affinity toxin binding derived from measurements of kinetic rate constants is in agreement with estimates for $\bar{K}'$. Absence of a distinct lag in association of radiotoxin with low-affinity sites is inconsistent with interconvertibility of sites.

The apparently coincident distribution of low-affinity and high-affinity toxin binding sites on rat brain membranes resolved by sedimentation velocity or density gradient centrifugation is consistent with, but not conclusive evidence for, their localization on the same patch of membrane, and perhaps on the same macromolecular complex. If so, then the apparent mismatch in toxin antagonistic potency and occupation of high-affinity toxin binding sites in ANS and CNS tisues may be explained. That is, blockade by antagonists of nicotinic cholinergic responses may require occupation of both low- and high-affinity toxin binding sites. At the neuromuscular junction, where toxin apparently binds with high affinity to all sites on nAcChoR, 100 nM toxin may be adequate to block cholinergic responses. However, for nAcChoR with low-affinity toxin binding sites (dissociation constants on the order of 100 nM), 50, 91, and 99% occupation will obtain at toxin concentrations of 100 nM, 1 μM, and 10 μM, respectively. The degree of functional blockade at these levels of receptor site occupation may vary with the cell type or system under investigation. If studies of ion flux across native sealed vesicles that contain *Torpedo* nAcChoR may be of predictive value, less than 20% of nAcChoR sites need be available to provide 10% of maximum ion flux (Lindstrom et al., 1980), which may in turn be adequate to trigger a full, postsynaptic cellular

response. Consequently, it is reasonable to expect that cholinergic response blockade in CNS and ANS tissues would require at least 1 μM toxin. Ligand competition experiments with d-TC and AcCho are consistent with the interpretation that both low- and high-affinity toxin binding sites have approximately the same affinities for AcCho and d-TC. Thus one would predict that agonistic potency of AcCho and antagonistic potency of d-TC would be identical for sites that bind toxin with low- or high-affinity, which is also consistent with pharmacological and physiological results reviewed above.

There are at least two potential caveats with this analysis. One is that investigations of *Torpedo* nAcChoR (Lindstrom et al., 1980) and muscle nAcChoR (Sine & Taylor, 1980, 1981) are consistent with inhibition of receptor function when only one of two toxin binding sites per nAcChoR monomer is occupied [however, see Delegeane & McNamee (1980) and Dunn et al. (1983)]. If one assumes a similar situation for nAcChoR in the ANS and CNS, then one must conclude that functional responses are activated through receptors that possess only low-affinity sites for toxin. Secondly, there is one laboratory that reports that Bgt at concentrations of 10 nM blocks nicotinic transmission in goldfish (Schmidt & Freeman, 1980) and toad (Freeman, 1977) optic tectum, consistent with the presence of only high-affinity (1 nM) toxin binding sites. Thus, there may be profound phylogenic differences in expression of nAcChoR with different affinities for toxin in the CNS, as well as in the ANS [see Chiappinelli et al. (1981)].

It should be pointed out that the existence of low-affinity toxin binding sites in chick ciliary ganglia was suggested by other investigators (Chiappinelli et al., 1981). Taken together with the present results, it is obvious that further examination of the functional relevance of CNS and ANS binding sites for curaremimetic neurotoxins, preferably in integral model systems that permit convergent studies of ligand binding and receptor function, is in order. More detailed biochemical studies are also indicated, in order to determine whether binding of radiotoxin is to noninteracting, noninterconvertible sites or to negatively cooperative sites or whether ternary complex (ligand–receptor–ligand or ligand–receptor–effector) formation is manifest. In addition, while the Scatchard-type plots exhibited are well fit to theoretical curves for high- and low-affinity sites present in approximately equal stoichiometry, dissociation ($\tau_{1/2} \simeq 1$ h) of radiotoxin from low-affinity sites during sample processing may lead to underestimates of the ratio of low- to high-affinity sites. Utilization of membrane preparations enriched in toxin binding sites and/or development of more rapid assay paradigms with adequate signal to noise ratios is critical to more rigorous analysis, under equilibrium conditions, of the low-affinity curaremimetic neurotoxin binding sites detected in the rat CNS.

Acknowledgments

I acknowledge the excellent technical assistance provided by Mary Jane Cullen and express appreciation to Deirdre Anne Janus for expert secretarial services.

Supplementary Material Available

Results and discussion pertaining to detection of low-affinity, toxin-resistant I-Bgt binding (5 pages). Ordering information is given on any current masthead page.

Registry No. α-Bungarotoxin, 11032-79-4.

References

Chiappinelli, V. A., Cohen, J. B., & Zigmond, R. E. (1981) *Brain Res. 211*, 107–126.
Chou, T. C., & Lee, C. Y. (1969) *Eur. J. Pharmacol. 8*, 326–330.
Conti-Tronconi, B. M., & Raftery, M. A. (1982) *Annu. Rev. Biochem. 51*, 491–530.
Delegeane, A. M., & McNamee, M. G. (1980) *Biochemistry 19*, 890–895.
Dun, N. J., & Karczmar, A. G. (1980) *Brain Res. 196*, 536–540.
Dunn, S. M. J., Conti-Tronconi, B. M., & Raftery, M. A. (1983) *Biochemistry 22*, 2512–1518.
Eterovic, V. A., & Bennett, E. L. (1974) *Biochim. Biophys. Acta 362*, 346–355.
Fex, J., & Adams, J. C. (1978) *Brain Res. 159*, 440–444.
Freeman, J. A. (1977) *Nature (London) 269*, 218–222.
Greene, L. A., Sytkowski, A. J., Vogel, Z., & Nirenberg, M. W. (1973) *Nature (London) 243*, 163–166.
Lee, C. Y. (1972) *Annu. Rev. Pharmacol. 12*, 265–286.
Lester, H. (1970) *Nature (London) 227*, 727–729.
Lindstrom, J., Anholt, R., Einarson, B., Engel, A., Osame, M., & Montal, M. (1980) *J. Biol. Chem. 255*, 8340–8350.
Lukas, R. J. (1984) *Biochemistry* (preceding paper in this issue).
Lukas, R. J., & Bennett, E. L. (1980) *Mol. Pharmacol. 17*, 149–155.
Lukas, R. J., Morimoto, H., & Bennett, E. L. (1979) *Biochemistry 18*, 2384–2395.
Lukasiewicz, R. J., Hanley, M. R., & Bennett, E. L. (1978) *Biochemistry 17*, 2308–2313.
Marshall, L. (1981) *Proc. Natl. Acad. Sci. U.S.A. 78*, 1948–1952.
Molinoff, P. B., Wolfe, B. B., & Weiland, G. A. (1981) *Life Sci. 29*, 427–443.
Moore, W. J., & Loy, N. J. (1972) *Biochem. Biophys. Res. Commun. 46*, 2093–2099.
Morley, B. J., & Kemp, G. E. (1981) *Brain Res. Rev. 3*, 81–104.
Norman, R. I., Mehraban, F., Barnard, E. A., & Dolly, J. O. (1982) *Proc. Natl. Acad. Sci. U.S.A. 79*, 1321–1325.
Oswald, R. E., & Freeman, J. A. (1981) *Neuroscience 6*, 1–14.
Romine, W. O., Goodall, M. C., Peterson, J., & Bradley, R. J. (1974) *Biochim. Biophys. Acta 367*, 316–325.
Salvaterra, P. M., & Moore, W. J. (1973) *Biochem. Biophys. Res. Commun. 55*, 1311–1318.
Schmidt, J., Hunt, S. P., & Polz-Tejera, G. (1980) in *Neurotransmitters, Receptors and Drug Action* (Essman, W. B., Ed.) pp 1–65, Spectrum, New York.
Schmidt, J. T., & Freeman, J. A. (1980) *Brain Res. 187*, 129–142.
Simantov, R., & Sachs, L. (1973) *Proc. Natl. Acad. Sci. U.S.A. 70*, 2902–2905.
Sine, S. M., & Taylor, P. (1980) *J. Biol. Chem. 255*, 10144–10156.
Sine, S. M., & Taylor, P. (1981) *J. Biol. Chem. 256*, 6692–6699.
Syapin, P. J., Salvaterra, P. M., & Engelhardt, J. K. (1982) *Brain Res. 231*, 365–377.
Zatz, M., & Brownstein, M. J. (1981) *Brain Res. 213*, 438–442.